Structural and electronic properties of crystalline and glassy calcium-zinc compounds. II.

Electronic density of states

Structural and electronic properties of crystalline and glassy calcium–zinc compounds: II. Electronic density of states

M Tegze† and J Hafner

Institut für Theoretische Physik, Technische Universität Wien,
Wiedner Hauptstrasse 8–10, A-1040 Wien, Austria

Abstract. We report self-consistent calculations of the electronic structure of crystalline and amorphous Ca–Zn alloys using a linearised muffin-tin orbital supercell method. Strong similarities between the electronic densities of state of the metallic glasses and the corresponding crystalline compounds are found. This supports previous conclusions from molecular dynamics studies of the atomic structure that the local order in the metallic glasses is similar to that in the trigonal prismatic inter-metallic compounds. In the Ca-rich phases the s,p conduction band splits into a fully occupied Zn 4s band and a valence band that is of pure 4p character on the Zn sites and of a strongly s,p,d-hybridised character on the Ca sites. The consequences of this result for the chemical bonding and the electronic properties are discussed.

1. Introduction

In the preceding paper [1] (hereafter referred to as I) we have studied the structural properties of amorphous Ca–Zn alloys using molecular dynamics simulations based on pseudopotential-derived inter-atomic forces. It was found that the static structure factor of the stable metallic glasses is characterised by a pre-peak. The origin of this pre-peak is in topological short-range order (TSRO). The investigation of the bond distances, bond angles and coordination numbers shows that this local order might be described as trigonal prismatic, in close analogy with the building principle of the crystalline compounds Ca_3Zn (Re_3B structure), Ca_5Zn_3 (Cr_5B_3 structure) and CaZn (CrB structure). In the present paper we supplement the investigation of the atomic structure by self-consistent calculations of the electronic density of states (DOS) for four Ca–Zn compounds in the crystalline and in the amorphous phase.

This work also continues a series of investigations of the electronic structure of simple-metal glasses [2–5]. In Mg–Zn glasses we had found a broad free-electron-like conduction band overlapping at its bottom with a narrow Zn 3d band and a small structure-induced minimum in the DOS at the Fermi level [2]. In Ca–Mg glasses the overall form of the DOS is again free electron like, but a possible structure-induced DOS

---

† On leave of absence from Central Research Institute for Physics, Hungarian Academy of Sciences, PO Box 49, H-1525 Budapest, Hungary.

minimum is covered by the onset of the Ca 3d states [3]. In Ca–Al glasses, strong electronic bonding effects lead to a pronounced deviation of the DOS from a free-electron form. The conduction band splits into a lower part dominated by Al 3s states and an upper part dominated by Al 3p states. Only the Al 3p states interact with the Ca states [4–5]. In any case the predictions of the electronic structure calculations are well confirmed by photoemission spectroscopy [2, 6, 7] and electronic specific heat measurements [8, 9]. In Ca–Zn glasses the electronic structure is complicated by all three factors:

(i) the Zn 3d band that will eventually overlap with the conduction band;
(ii) the onset of the Ca 3d states at the Fermi level;
(iii) strong electronic bonding effects due to the large difference between the electron densities of Ca and Zn.

In addition the pronounced TSRO will eventually be reflected in the DOS.

Our paper is organised as follows. In § 2 we recapitulate very briefly the technical aspects of the linearised muffin-tin orbital (LMTO) supercell method, in § 3 we present the calculated DOS for the crystalline and amorphous compounds, and in § 4 we summarise the results of the investigation of the structural and electronic properties.

2. Linearised muffin-tin orbital supercell method

The methods available for the calculation of the electronic DOS fall into three categories:

(i) effective-medium techniques;
(ii) equation-of-motion or recursion calculations;
(iii) cluster and supercell calculations.

Our reasons for adopting a supercell method and in particular the LMTO method in the atomic-sphere approximation (ASA) [10, 11] have been given in our previous papers [2, 3]. The main advantage of the supercell method is that it allows for a locally self-consistent calculation of the electronic structure—thus it is well suited to studying the interplay of the atomic and the electronic structure in amorphous materials. The main limitations arise from the relatively small number of atoms per periodically repeated supercell. The molecular dynamics method for the modelling of the amorphous structure has been described in I. Simulations for large ensembles (1372 atoms in a periodically repeated cubic box) have been performed to produce correlation functions with good statistical accuracy. Parallel to these runs we have carried out simulations with small ensembles (64 atoms). The configurations generated in these runs form the basis for the electronic structure calculations. In figure 1 we compare the partial correlation functions $g_{ij}(R)$ for amorphous CaZn and Ca_3Zn, calculated from a single 64-atom configuration and obtained by averaging over 100 independent 1372-atom configurations. We find that even for the minority atoms all the relevant features of the correlation functions are reasonably well reproduced by the 64-atom ensemble so that this really is a relevant structural model.

Usually supercell calculations are done for the Γ point (in practice, for $k = (0.0, 0.0, 0.01)$ (π/a) of the Brillouin zone of the simple-cubic supercell only [12, 13], and a continuous DOS is derived from the discrete spectrum of the Γ-point eigenvalues by an appropriate Gaussian broadening. This works well for the relatively narrow bands of transition-metal and rare-earth systems. In a divalent simple-metal glass the situation is different; with 64 atoms per cell, only 128 occupied Γ-point eigenvalues are distributed
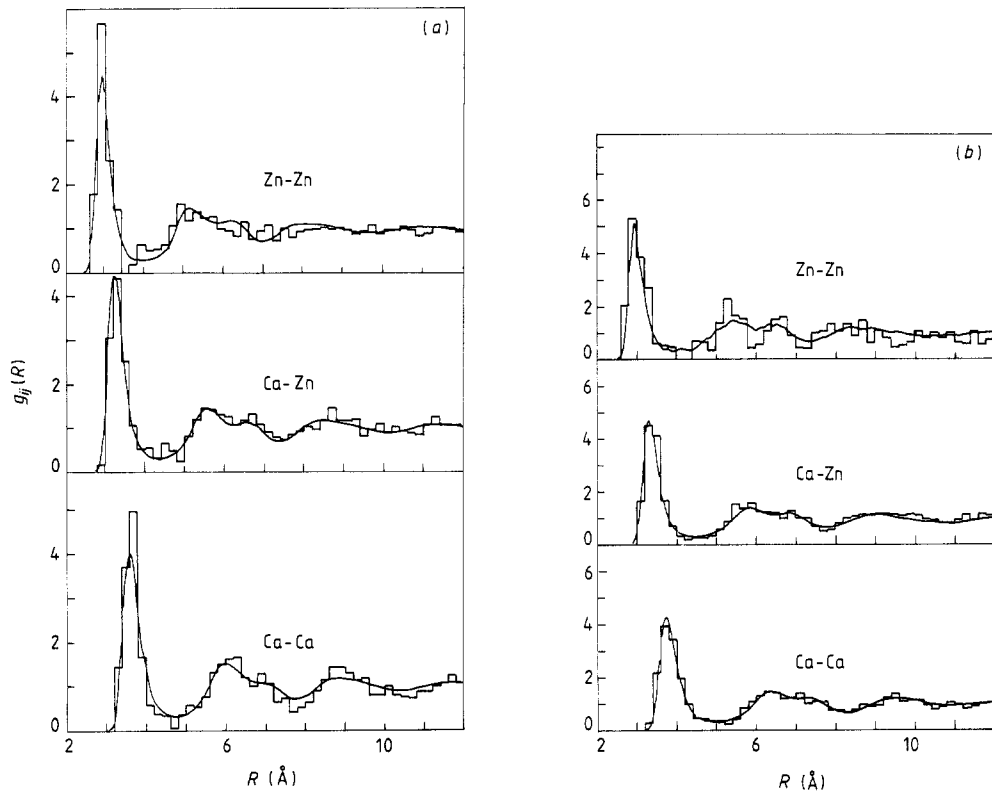
Figure 1. Partial pair correlation functions $g_{ij}(R)$ for amorphous (*a*) CaZn and (*b*) Ca$_3$Zn: ———, correlation functions resulting from an ensemble average over 100 independent configurations of a 1372-particle ensemble; the histogram shows the pair correlations in a single 64-atom calculation used in the electronic structure calculation.

over a band that is about 10 eV wide, and with a modest Gaussian broadening (we use a Gaussian with a width of 0.2 eV) this produces a DOS with spurious structures [2, 3]. If we sample the eigenvalues from four Brillouin zone points (we take the corners of the irreducible wedge), most of the unphysical structure disappears. A further extension to 10 *k*-points does not significantly alter the DOS. The alternative to an increase in the number of *k*-points would be to enhance the number of atoms per supercell. However, even with twice as many atoms per cell, the cube edge of the supercell increases only by one inter-atomic distance; therefore the convergence is expected to be slow and the computational effort very high. It is true that the extended *k*-point average neglects the structural disorder beyond the 64-atom cell; hence it is necessary to have at least an estimate of the influence of the periodic boundary conditions. This point has been investigated in [5] for Ca$_7$Al$_3$ via a comparison of the results of a 60-atom LMTO supercell calculation with those of an 800-atom tight-binding (TB) LMTO recursion calculation. The TB LMTO parameters have been calculated from the final self-consistent potential of the supercell calculations. The results of both calculations are in good agreement, demonstrating that the supercell result is not seriously affected by the periodic boundary conditions.

In principle the DOS has to be averaged over a number of independent configurations. However, in all our previous studies we had found that the DOS from a single 64-atom calculation yields a representative picture.

For the crystalline compounds, we used the standard LMTO ASA, the DOS was calculated using the linear tetrahedron method [14, 15].

3. Electronic density of states of crystalline and amorphous Ca–Zn compounds

The detailed crystallographic description of the crystalline inter-metallic Ca–Zn phases has been given in I (tables 1–5). This paper also contains information on the amorphous structures.

3.1. CaZn$_5$

Crystalline CaZn$_5$ has the structure of a hexagonal Frank–Kasper phase with five atoms in the primitive cell (see table 2 and figure 2 of I). The ratio R_{Ca}/R_{Zn} of the atomic sphere radii was taken to be 1.42; the DOS is calculated from 112 k-points in the irreducible part of the Brillouin zone. The total, site-decomposed and angular-momentum-decomposed electronic DOSs are shown in figure 2. The general form is very similar to that of pure HCP Zn; a narrow Zn 3d band (the width W at half-maximum is 1.7 eV; in pure Zn, one finds that $W = 1.82$ eV) is centred at $E_{3d}^{Zn} = 7.4$ eV below the Fermi level, i.e. exactly at the same binding energy as in pure Zn. The Zn 3d band overlaps with the bottom of the conduction band which is considerably broadened relative to the free-electron value through the s–d hybridisation. The most prominent structure in the conduction band is the deep minimum just above E_F, which is also found in pure HCP Zn. This is a structure-induced minimum; it is clearly associated with the fact that the Zn atoms form a tetrahedrally close-packed array both in the pure metal and in the inter-metallic compound. The conduction band shows the strong s,p,d mixing characteristic of free-electron-like simple-metal systems; the Ca-based bands are considerably broadened through the interaction with the Zn states.

3.2. CaZn$_2$

Crystalline CaZn$_2$ assumes the orthorhombic CeCu$_2$ structure with 12 atoms/cell (see table 3 and figure 3(c) of I). The structure can be described as a dense three-dimensional packing of distorted trigonal Ca prisms centred by Zn. In the LMTO calculations the ratio R_{Ca}/R_{Zn} of the atomic sphere radii is taken to be 1.42; the DOS integration is based on 120 k-points in the irreducible Brillouin zone.

The DOS for the crystalline CaZn$_2$ is shown in figure 3(a). The Zn 3d band is now much narrower ($W = 0.75$ eV); its centre of gravity has been shifted to slightly lower binding energy ($E_{3d}^{Zn} = 7.2$ eV). The conduction band DOS shows stronger structure than that of the hexagonal Laves phases MgZn$_2$ [2] or CaMg$_2$ [3]. The s,p,d hybridisation is considerably reduced; the lower part of the band with a prominent peak at 5 eV binding energy is dominated by the Zn 4s states, and the upper part with a double-peaked maximum just at E_F by the Zn 4p states. The Ca 4s and Ca 4p states contribute mainly to the upper part of the band that lies between 4 eV binding energy and E_F. At the Fermi level the partial Ca DOS is mainly of p and d character; thus there are clear indications for an inter-atomic s $\rightarrow$ d promotion as in CaAl$_2$ and in pure Ca under pressure. The
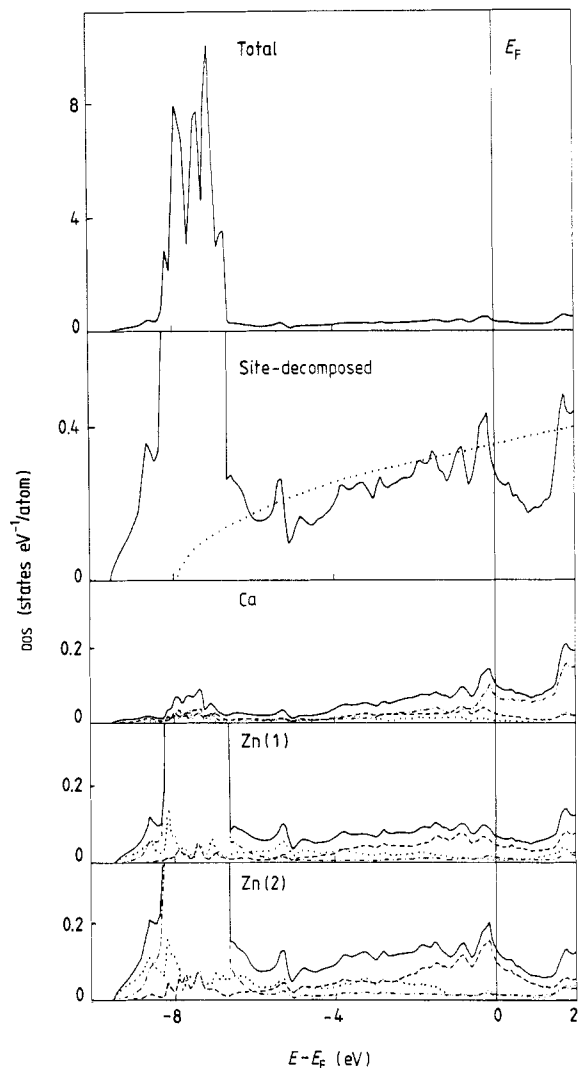
Figure 2. Total, site-decomposed and angular-momentum-decomposed DOSs for crystalline $CaZn_5$: ———, total DOS; · · · ·, partial s DOS; — — —, partial p DOS; — · —, partial d DOS. The dotted curve in the enlarged graph of the total DOS shows the free-electron DOS for comparison.

incipient dehybridisation of the Zn conduction states is clearly related to the atomic structure; at an approximately constant Zn–Zn bond length, the number of direct Zn–Zn neighbours is reduced from 12 in the pure metal to four in the $CaZn_2$ compound (see table 6 in I). The reduced overlap leads to a narrowing of all sub-bands. This tendency is enhanced by the chemical short-range order (preferred heterocoordination) in this compound.

The DOS for the amorphous $CaZn_2$ alloy is essentially a smoothened version of the crystalline DOS (figure 3(b)). The Zn 3d band is broadened ($W \simeq 1$ eV) and shifted to a slightly higher binding energy ($E_{3d}^{Zn} = 7.5$ eV). The structures in the conduction band associated with the van Hove singularities of the complex crystal lattice have disappeared, but the maxima at 4–5 eV and at E_F, close to the centres of gravity of the s and p bands persist. Again the lower part of the Ca DOS contains equal amounts of all three angular momentum components; this suggests that the origin of the Ca DOS at these energies is mainly in the overlap of the extended Zn 4s orbitals into the neighbouring Ca
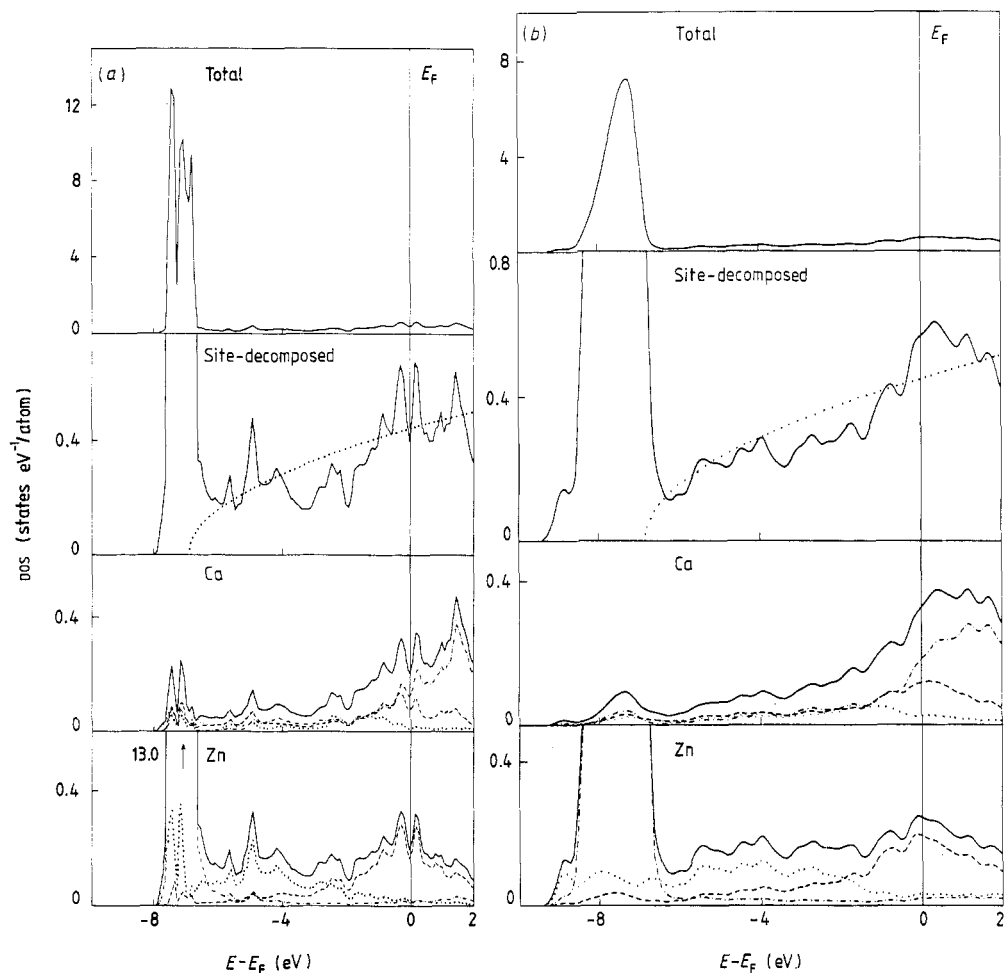
Figure 3. Total, site-decomposed and angular-momentum-decomposed DOSS for (a) crystalline and (b) amorphous $CaZn_2$: for meanings of symbols see figure 2.

spheres. Altogether the consideration of the electronic structure confirms the conclusion drawn from the analysis of the atomic structure model; the local order and bonding are very similar in the crystalline and in the amorphous alloys.

3.3. CaZn

CaZn crystallises in the CrB structure (see table 4 and figure 3(b) of I). This structure is assumed by many transition-metal borides, phosphides and carbides, and by many compounds of the heavy alkaline-earth elements (Ca, Sr and Ba) with the group IV elements, with the noble metals and with Ga and Zn [16, 17]. For the IIA–IVB compounds the origin of this structure is usually explained in terms of conventional chemical bond theory; even if the alkaline-earth atoms donate all their valence electrons to the IVB atoms, two anions still have to share an electron pair to complete an octet shell and this is thought to stabilise the anion zigzag chains via $pp\sigma$ bonds. However, of course
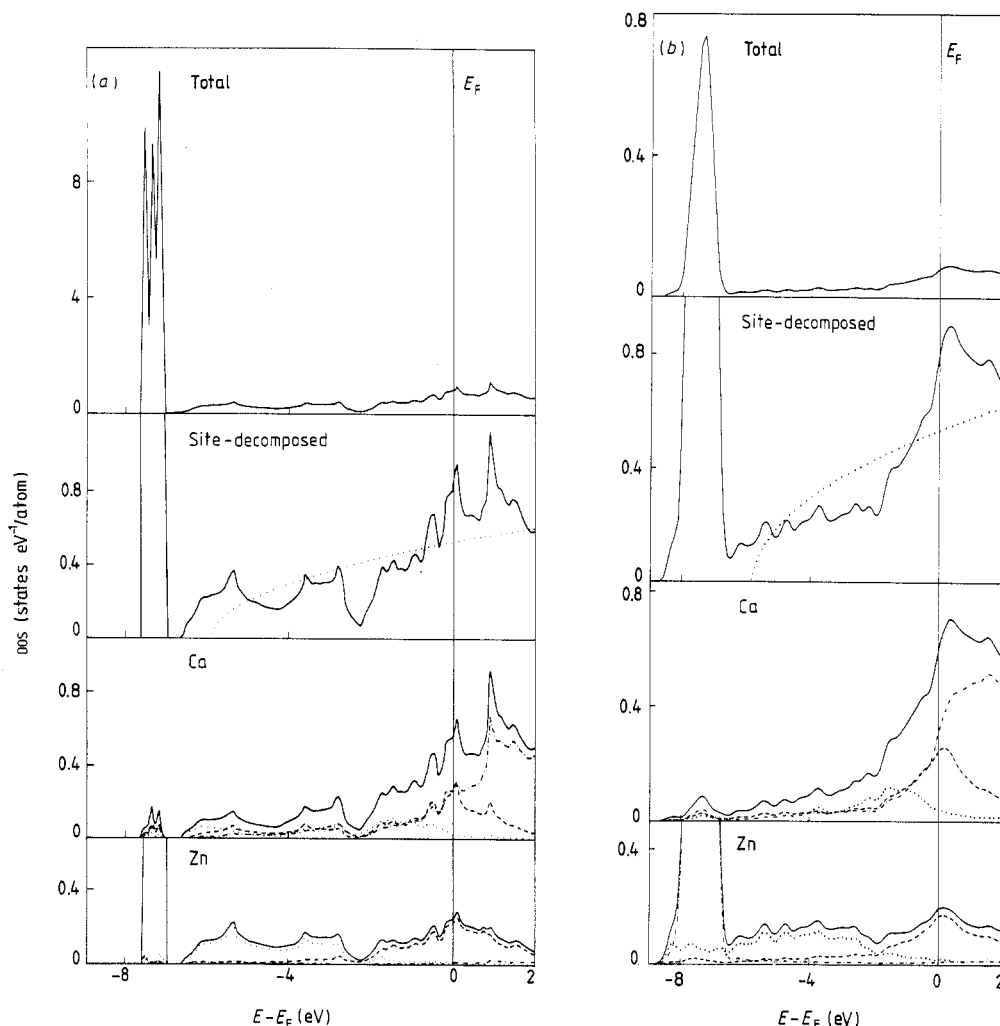
Figure 4. Total, site-decomposed and angular-momentum-decomposed densities of state for (*a*) crystalline and (*b*) amorphous CaZn: for meanings of symbols see figure 2.

such a simple electron-counting rule cannot hold for the IIA–IIB compounds and there are also small but significant differences in the structure. In the IIA–IVB phases the trigonal prisms are stretched (indicating weak IIA–IIA bonds), while they are compressed in the IIA–IIB and IIA–IB phases [16].

The electronic DOS for crystalline CaZn is shown in figure 4(*a*). The ratio R_{Ca}/R_{Zn} of the atomic sphere radii was chosen as 1.47; 100 *k*-points were used for the calculation of the DOS. The narrow Zn 3d band ($W \approx 0.5$ eV; $E_{3d}^{Zn} = 7.3$ eV) is now completely separated from the conduction band. In the conduction band we find a very deep minimum (almost a gap) at 2.3 eV. The lower part of the band is of nearly pure 4s character on the Zn sites, and of a completely mixed character on the Ca sites. This means that the Ca DOS stems mainly from the overlap of the extended Zn 4s orbitals into the Ca spheres and that the band is in reality a Zn 4s band. This assertion is confirmed by the fact that

the band contains exactly two electrons per zinc atom. Thus it is a fully occupied non-bonding band. The upper part of the conduction band consists of Zn 4p and Ca s,p,d states. Part of the Ca DOS—in particular at the lower edge of the band—might be due to overlapping Zn states. At the Fermi level, p and d states dominate the Ca DOS; the onset of the Ca 3d DOS leads to a DOS at E_F which is considerably enhanced over the free-electron value.

Altogether we find that the electronic structure is dominated by the electronegative Zn atoms. This is not too surprising, since they also have the more attractive electron–ion potential. Similar situations have been found in the Ca-based Laves phases [3, 4, 18] and in several alkali–lead compounds [19]. Even if the octet rule cannot be satisfied, the Zn–ppσ bond still play an essential role in stabilising the Zn–Zn chains in the CrB structure. The form of the partial Ca s,p,d DOSs points to a large inter-atomic s $\rightarrow$ d promotion. Thus Ca in CaZn behaves almost as a transition metal. This makes the simultaneous occurrence of this crystal structure in the transition-metal borides and in the IIA–Zn compounds at least plausible. The structural differences between the IIA–Zn and the IIA–IVB phases originate from the greater importance of the bonding between the alkaline-earth atoms in the CaZn compound.

In the amorphous phase (figure 4(*b*)) the pseudo-gap almost disappears through the general broadening of the electronic DOS. From the partial DOSs, however, we learn that the character of the bands remains the same; the electron states between 2 and 7 eV binding energy form a non-bonding Zn 4s band which overlaps with the Zn 3d band at its lower end and the bonding part of the conduction band at its upper end. The bonding states close to E_F are again dominated by Zn 4p, Ca 4p and Ca 3d states. This indicates that the role of the Zn–ppσ bonds is preserved in the amorphous state.

In this context we should remember that the structure factors of the computer-generated models for amorphous CaZn and amorphous Ca_3Zn show a pre-peak in the Zn–Zn partial structure factor and in the number-density structure factor indicating TSRO associated with strong Zn–Zn correlations (see § 4 in I). The electronic structure calculations described here certainly support our suggestion that this is an indication of trigonal prismatic order in amorphous CaZn.

3.4. Ca_3Zn

The Ca_3Zn compound crystallises in the orthorhombic Re_3B structure (see table 5 of I). Again the Zn atoms lie at the centre of trigonal Ca prisms which are arranged in chains running parallel to the *a* axis (see figure 3 of I). The ratio R_{Ca}/R_{Zn} of the atomic sphere radii is taken to be 1.47; 72 *k*-points are used in the Brillouin zone integration. The systematic trends in the electronic structure of the crystalline Ca–Zn compounds are continued in Ca_3Zn (figure 5(*a*)). The Zn 4s band is separated by a gap (0.6 eV wide) from the conduction band which is again of pure 4p character on the Zn sites and has p–d character on the Ca sites. The total DOS of the conduction band is already quite similar to that of pure Ca except for a small s $\rightarrow$ d promotion. This is not surprising since the volume per Ca atom is only 7.5% larger than in pure Ca and the average coordination number is also almost the same ($N_c = 11.3$ as against $N_c = 12$ in FCC Ca; see table 6 of I). The Zn 4p contribution to the DOS at E_F suggests that there is an appreciable ppσ bonding along the straight Zn chains which contributes to the stability of the compound.

In the glassy Ca_3Zn phase the energy gaps between the sub-bands are covered by a diffuse background arising from the strong structural disorder in the system which also leads to a smearing of the details of the DOS. However, this does not destroy the
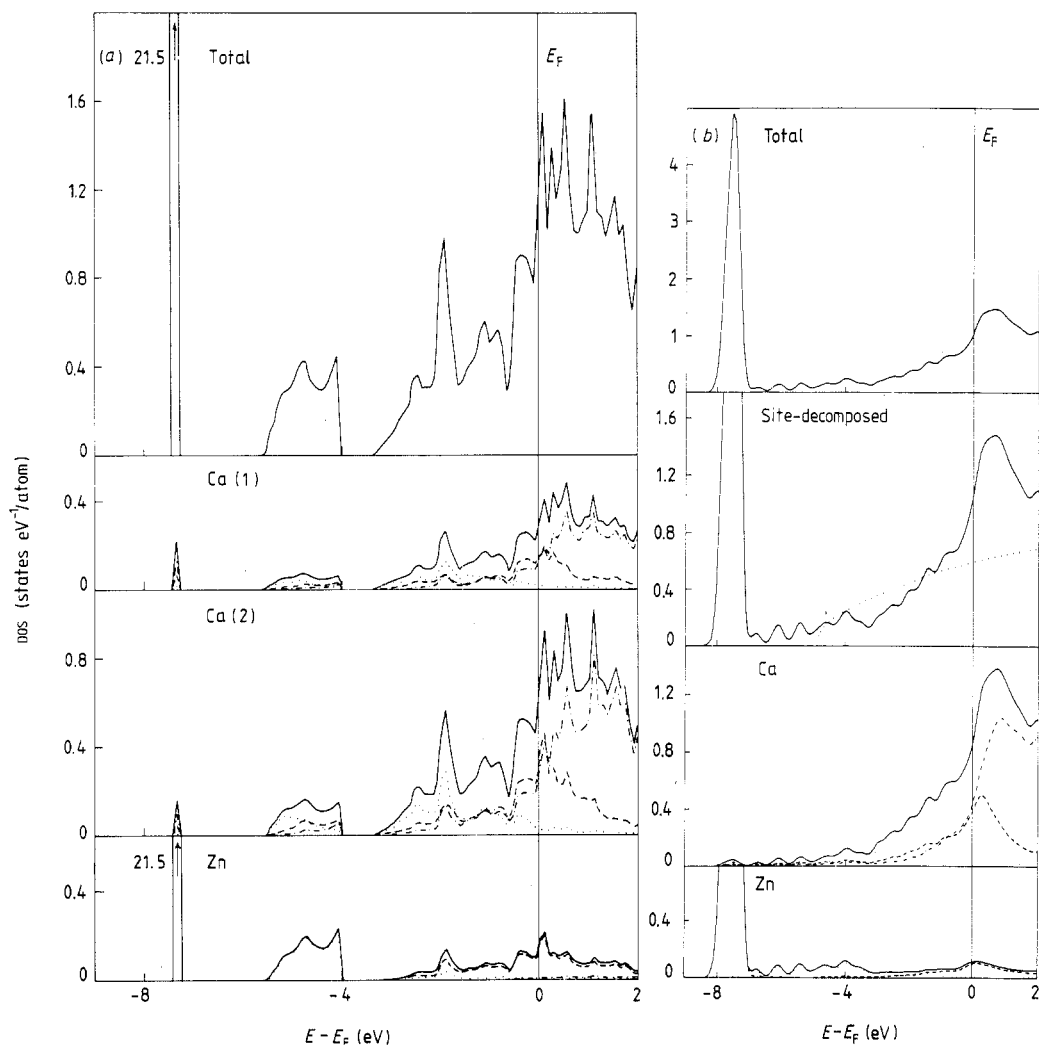
Figure 5. Total, site-decomposed and angular-momentum-decomposed DOSs for (*a*) crystalline and (*b*) amorphous CaZn$_3$: for meanings of symbols see figure 2.

characteristic features of the conduction band: splitting into a non-bonding Zn 4s band and a bonding band with a pure 4p character on the Zn sites and a strong d character on the Ca sites. From the form of the partial Ca DOS it is very clear that the 'real' conduction band onset is at 3.3 eV (i.e. precisely at the lower edge of the Zn 4p DOS) and that all Ca states found at higher binding energies are merely resonances. Again the DOS at the Fermi level is strongly enhanced over the free-electron value.

4. Conclusions

We have presented self-consistent calculations of the electronic structure of crystalline and amorphous Ca–Zn alloys. Our results are compatible with the conclusion drawn

from the investigation of the atomic structure; the local order in the stable Ca–Zn glasses is very similar to that in the trigonal prismatic inter-metallic compounds. The most characteristic feature of the electronic structure of the crystalline compounds CaZn and Ca_3Zn is the splitting of the s,p band of the pure metals into a completely filled non-binding Zn 4s band and a relatively narrow conduction band ($W = 3.4$ eV in Ca_3Zn, and $W = 2.3$ eV in CaZn) consisting of Zn 4p states and strongly s,p,d-hybridised Ca states. The strong p character of the Zn conduction band supports old ideas on the bonding in CrB-type inter-metallic phases (ppσ bonds along the B(Zn) chains), even though in Ca–Zn there are not enough electrons to satisfy the 8-N rule.

It is important to relate these results to the inter-atomic potentials which are the basis of the computer simulations described in I. There we have shown that in Ca–Zn alloys the variation in the screening function and in the core orthogonalisation effects with composition leads to a more attractive Zn pseudopotential and to a stronger Zn–Zn pair interaction than in pure Zn. The change in the orthogonalisation affects the s component more than the p component. This is just what the electronic structure calculations give for the partial Zn DOS: stronger s bonding and comparatively weaker p and d bonding with increasing Ca content. Conversely on the Ca sites the d-electron bonding is strengthened at the expense of s- and p-electron bonding. Thus pseudopotential perturbation calculations and the LMTO determination of the electronic DOS offer a consistent picture.

The main features of the electronic DOS of the crystalline compounds are preserved in the metallic glasses and should be verifiable by experiment.

(i) The electronic DOS at the Fermi level is strongly enhanced over the free-electron value.

(ii) The splitting of the s,p band should be observable in a good photoemission experiment. However, the interpretation of these experiments will not be straight-forward. We expect photoelectron spectroscopy to show a relatively large shift of the narrow Zn 3d band due to self-energy effects. Such a d-band shift has been observed in amorphous Mg–Zn alloys. We have shown that it can be explained by a transition-state analysis [2].

(iii) As the Zn 4s is nearly completely separated from the rest of the conduction band, we would expect Zn 4s electrons not to contribute to the electronic transport. This should result in a Hall constant that is considerably more negative than the free-electron value and a relatively high electrical resistivity.

We have been informed that experimental investigations of the electronic structure and transport properties are now in process and will soon be published [20].

We find that compared with other Ca-based metallic glasses the electronic structure of Ca–Zn glasses is intermediate between that of the weak-scattering Ca–Mg and the strong-scattering Ca–Al glasses: strong enhancement of the DOS at E_F as in Ca–Mg (but not Ca–Al), and dehybridisation of the Zn s,p states (as in the Al s,p states in Ca–Al).

References

[1] Hafner J and Tegze M 1989 *J. Phys. Condens. Matter* **1** 8277–91
[2] Hafner J, Jaswal S S, Tegze M, Pflugi A, Krieg J, Oelhafen P and Güntherodt H J 1988 *J. Phys. F: Met. Phys.* **18** 2583
[3] Jaswal S S and Hafner J 1988 *Phys. Rev.* B **38** 7311
[4] Hafner J and Jaswal S S 1988 *Phys. Rev.* B **38** 7320
[5] Bose S K, Jaswal S S, Andersen O K and Hafner J 1988 *Phys. Rev.* B **37** 9955
[6] Nagel S R, Gubler U, Hague C F, Krieg J, Lapka R, Oelhafen P, Güntherodt H J, Evers J, Weiss A, Moruzzi V L and Williams A R 1983 *Phys. Rev. Lett.* **49** 57
[7] Mizutani U and Oelhafen P 1989 private communication
[8] Mizutani U and Matsuda T 1985 *Proc. 5th Int. Conf. Rapidly Quenched Metals* vol 1, ed. S Steeb and H Warlimont (Amsterdam: North-Holland) p 1035
[9] Mizutani U, Sasaura M, Yamada Y and Matsuda T 1987 *J. Phys. F: Met. Phys.* **17** 667
[10] Andersen O K, Jepsen O and Glötzel D 1985 *Highlights of Condensed Matter Theory* ed. F Bassani, F Fumi and M P Tosi (Amsterdam: North-Holland)
[11] Skriver H L 1981 *Springer Series in Solid State Sciences* vol 41 (Berlin: Springer)
[12] Jaswal S S 1986 *Phys. Rev.* B **34** 8937
[13] Jaswal S S, Sellmyer D J, Engelhardt M, Zhao Z, Arko A J and Xie K 1987 *Phys. Rev.* B **35** 996
[14] Jepsen O and Andersen O K 1971 *Solid State Commun.* **9** 1762
[15] Lehmann G and Taut M 1972 *Phys. Status Solidi* b **54** 469
[16] Fornasini M L 1985 *J. Solid State Chem.* **59** 60
[17] Parthé E 1981 *Structure and Bonding in Crystals* vol II, ed. M O'Keefe and A Navrotsky (New York: Academic) p 259
[18] Hafner J 1989 *Cohesion and Structure* vol 2 *The Structures of Binary Compounds* ed. D G Pettifor and F R de Boer (Amsterdam: North-Holland) ch 3
[19] Tegze M and Hafner J 1989 *Phys. Rev.* B **39** 8263
[20] Mizutani U 1989 private communication